

Extrinsic Optical Scattering Loss in Photonic Crystal Waveguides: Role of Fabrication Disorder and Photon Group Velocity

S. Hughes*

NTT Basic Research Laboratories, NTT Corporation, Atsugi, Japan

L. Ramunno[†]

Department of Physics, University of Ottawa, Ottawa, Canada

Jeff F. Young

Department of Physics and Astronomy, University of British Columbia, Vancouver, Canada

J. E. Sipe

Department of Physics, University of Toronto, Toronto, Canada

(Received 28 April 2004; published 25 January 2005)

Formulas are presented that provide clear physical insight into the phenomenon of extrinsic optical scattering loss in photonic crystal waveguides due to random fabrication imperfections such as surface roughness and disorder. Using a photon Green-function-tensor formalism, we derive explicit expressions for the backscattered and total transmission losses. Detailed calculations for planar photonic crystals yield extrinsic loss values in overall agreement with experimental measurements, including the full dispersion characteristics. We also report that loss in photonic crystal waveguides scales inversely with group velocity, at least, thereby raising serious questions about future low-loss applications based on operating frequencies that approach the photonic band edge.

DOI: 10.1103/PhysRevLett.94.033903

PACS numbers: 42.70.Qs, 41.20.Jb, 42.25.Fx, 42.65.-k

Light scattering is one of the most important physical mechanisms dictating the characteristics of light propagation and confinement in sub-wavelength-scale nanostructures. In this regard, the unique properties of light scattering in periodic media are the defining feature of photonic crystals (PCs) [1]. Appropriately engineered coherent scattering in PCs can give rise to exciting new applications and novel fundamental physics, many of which come about because the propagating light can be slowed down. However, uncontrolled scattering can also be very detrimental, i.e., by contributing to optical losses. In particular, *extrinsic* scattering loss resulting from random fabrication variations, such as disorder and surface roughness, is now regarded as one of the most critical hurdles facing the development of PCs and PC devices. This is partly evidenced by an increasing number of experiments [2–4] that measure typical losses in planar photonic crystal (PPC) waveguides to be orders of magnitude larger than competing nanoscale waveguides. This is true even with state-of-the-art fabrication techniques that produce only nm-size surface roughness. In addition, recent experiments have shown that loss in PC waveguides is highly dispersive [5,6], and there are some frequency ranges in which the loss is unusually large, even for bound modes below the light line. Despite its importance, and while much effort has been devoted to the characterization of ideal (lossless) PC and PPC waveguides [1,7], there has been little theoretical work describing extrinsic scattering loss in PC and PPC waveguides and microcavities.

Scattering theory for regular optical waveguides with rough surfaces, however, has been around for quite some time. In the pioneering work of Marcuse [8], explicit expressions for loss were obtained that scale quadratically with both the electric field strength and the change in electric permittivity across the sidewalls, multiplied by a fairly complicated integral over radiation modes. This formalism was simplified considerably by Payne and Lacey [9] who related the integral to physically relevant parameters such as rms roughness and spatial correlation lengths.

In the domain of PC waveguides, there have been only a few theoretical investigations of out-of-plane scattering losses, but many of these focus on intrinsic scattering loss, i.e., diffraction loss for inherently leaky modes [10–12], and do not address extrinsic, disorder-induced scattering. The little previous work there is on extrinsic loss has dealt with only very specific structures and/or types of disorder, including systematic numerical investigations [13], 2D infinitely long cylinders [14] and layered structures [15], and out-of-plane structural asymmetries [16]. None of these extrinsic loss studies present methods or equations that allow sufficient physical insight or that are general enough to determine loss in arbitrary PC waveguides. In this Letter we present a formalism that yields explicit formulas for both the backscattered and total transmission loss for arbitrary PC waveguides with a wide range of disorder imperfections [17].

Our approach begins with the lossless Bloch mode of a perfect PC waveguide described by the ideal dielectric

function $\epsilon_B(\mathbf{r})$. To facilitate a photon Green-function-tensor (GFT) solution that captures the effect of random variations contained in the true dielectric function $\epsilon_t(\mathbf{r})$, we define a disorder function by $\Delta\epsilon = \epsilon_t - \epsilon_B$. A general solution for the electric field is $\mathbf{E}(\mathbf{r}; \omega) = \mathbf{E}^B(\mathbf{r}; \omega) + \int d\mathbf{r}' \vec{\mathbf{G}}^B(\mathbf{r}, \mathbf{r}'; \omega) \cdot \Delta\epsilon(\mathbf{r}') \mathbf{E}(\mathbf{r}'; \omega)$, where \mathbf{E}^B is the unperturbed electric field for the propagating Bloch mode, and $\vec{\mathbf{G}}^B$ is the ideal GFT of the PC structure obtained through a solution of Maxwell equations with an oscillating dipole source. In principle, one can then solve for \mathbf{E} exactly. The corresponding numerical calculation, however, would involve solving a self-consistent matrix equation over sizes impractical (and unnecessary) for our present purpose. Instead we derive simple yet valid expressions for extrinsic loss, by making a second-order Born approximation, giving $\mathbf{E}(\mathbf{r}; \omega) = \mathbf{E}^B(\mathbf{r}; \omega) + \int d\mathbf{r}' \vec{\mathbf{G}}^B(\mathbf{r}, \mathbf{r}'; \omega) \cdot \Delta\epsilon(\mathbf{r}') \mathbf{E}^B(\mathbf{r}'; \omega) + \iint d\mathbf{r}'' \times d\mathbf{r}' \vec{\mathbf{G}}^B(\mathbf{r}, \mathbf{r}'; \omega) \cdot \Delta\epsilon(\mathbf{r}') \vec{\mathbf{G}}^B(\mathbf{r}', \mathbf{r}''; \omega) \cdot \Delta\epsilon(\mathbf{r}'') \mathbf{E}^B(\mathbf{r}''; \omega)$.

We obtain our PC loss formulas by first seeking expressions for the reflectivity and transmissivity of the waveguide bound modes. We also represent the GFT by a sum of a bound contribution in terms of the waveguide bound modes, and a separate contribution that contains everything else, such as radiation modes. We assume our waveguide is periodic along the direction of propagation x with period a and is single mode at frequency ω . Applying Bloch's theorem, the bound contribution to the GFT is expressed analytically as $\vec{\mathbf{G}}_k^B(\mathbf{r}, \mathbf{r}'; \omega) = i0.5a\omega/|v_g|[\mathbf{e}_k(\mathbf{r}) \otimes \mathbf{e}_k^*(\mathbf{r}') e^{ik(x-x')} \Theta(x-x') + \mathbf{e}_k^*(\mathbf{r}) \otimes \mathbf{e}_k(\mathbf{r}') e^{-ik(x-x')} \Theta(x'-x)]$, with \mathbf{e}_k the forward propagating Bloch mode for wave number k at ω such that $\mathbf{E}_k \propto \mathbf{e}_k e^{ikx}$, v_g is the associated group velocity, Θ is the Heaviside step function, and the normalization $\int_{\text{cell}} |\mathbf{e}_k(\mathbf{r})|^2 \epsilon(\mathbf{r}) d\mathbf{r} = 1$ is carried out over one unit cell of the periodic structure. The group velocity appears by carrying out a complex integration over the bound mode dispersion [17].

Combining $\vec{\mathbf{G}}_k^B$ with the expression for \mathbf{E} , we derive transmission and reflection coefficients by taking the limits $\mathbf{r} \rightarrow \pm\infty\hat{x}$, retaining terms only to second order in $\Delta\epsilon$. These lead to our main results: formulas for the backscatter and total transmission power loss [18]

$$\alpha_{\text{back}}(\omega) = \frac{a^2 \omega^2}{4|v_g|^2} \iint d\mathbf{r} d\mathbf{r}' \Delta\epsilon(\mathbf{r}) \Delta\epsilon(\mathbf{r}') [\mathbf{e}_k^*(\mathbf{r}) \cdot \mathbf{e}_k^*(\mathbf{r}')] \times [\mathbf{e}_k(\mathbf{r}') \cdot \mathbf{e}_k(\mathbf{r}')] e^{i2k(x-x')}, \quad (1)$$

$$\alpha_{\text{total}}(\omega) = \frac{a\omega}{|v_g|} \iint d\mathbf{r} d\mathbf{r}' \Delta\epsilon(\mathbf{r}) \Delta\epsilon(\mathbf{r}') \text{Im}\{\mathbf{e}_k^*(\mathbf{r}) \cdot \vec{\mathbf{G}}^B(\mathbf{r}, \mathbf{r}'; \omega) \cdot \mathbf{e}_k(\mathbf{r}') e^{ik(x-x')}\}. \quad (2)$$

The out-of-plane loss is simply $\alpha_{\text{total}} - \alpha_{\text{back}}$. The presence of $\Delta\epsilon$ ensures that only regions containing imperfections contribute to the loss. We see immediately from Eqs. (1) and (2) that loss grows as $v_g \rightarrow 0$, i.e., when the

waveguide mode frequency approaches the photonic band gap, capturing the same trend observed in experiments on PPC waveguides [5,19]. A smaller v_g means that light moves more slowly through the waveguide and thus has more time to sample the regions of disorder and roughness.

To proceed with numerical calculations, first one calculates the GFT, the Bloch function, and v_g for the ideal structure; to accomplish this we use our own finite-difference time-domain [20] techniques, which will be described in a future publication. Second, one needs a model for $\Delta\epsilon$ based on the particular imperfections and fabrication process that best represent the waveguide under study. The properties of $\Delta\epsilon$ that we consider here are for PPCs where the patterning is accomplished through an etching procedure. Typically, the dominant imperfection is surface roughness appearing on the sidewalls of the patterned features, rather than disorder due to incorrect feature positioning [19]. Thus, we account for correlations along the surface of the etched air-dielectric boundaries but assume that disorder between distinct etched features and along surfaces between the multilayers is uncorrelated. In most etched semiconductors, roughness occurs due to random fabrication variations in the mask. After etching, this translates to vertical striations appearing on the sidewalls of the patterned features. It is reasonable, then, to assume perfect correlation in the vertical direction, so we need only address in-plane variations.

Our example structure is a semiconductor membrane with a number of etched holes (α) of radius R with centers located at the points $\boldsymbol{\rho}_\alpha$, where $\boldsymbol{\rho} = (\rho, \phi)$ is the in-plane coordinate. The vertical coordinate is z and the membrane height is h . An exact expression for $\Delta\epsilon$ can be written in terms of a roughness function ΔL , defined as the distance between the true and ideal structures. For a hole centered at the origin, ΔL is simply a function of ϕ . For a hole centered at $\boldsymbol{\rho}_\alpha$, ΔL is a function of a translated angle coordinate $\tilde{\phi}(\boldsymbol{\rho}, \boldsymbol{\rho}_\alpha) = \arctan[(\rho \sin\phi - \rho_\alpha \sin\phi_\alpha)/(\rho \cos\phi - \rho_\alpha \cos\phi_\alpha)]$. In the limit $\Delta L \ll R$ one can write, for multiple holes, $\Delta\epsilon(\mathbf{r}) = (\epsilon_2 - \epsilon_1) \times \Theta(h/2 - |z|) \sum_\alpha \Delta L(\tilde{\phi}(\boldsymbol{\rho}, \boldsymbol{\rho}_\alpha)) \delta(R - |\boldsymbol{\rho} - \boldsymbol{\rho}_\alpha|)$, where ϵ_1 (ϵ_2) is the dielectric constant in the etched layer outside (inside) the air holes. While the best method of determining the statistics of ΔL is certainly through direct measurement, this is not always possible. Instead, we calculate the ensemble averages of Eqs. (1) and (2) by employing a version of a well-established multiple-scattering correlation function [9] $\langle \Delta L(\tilde{\phi}) \Delta L(\tilde{\phi}') \rangle = \sigma^2 e^{-R|\tilde{\phi} - \tilde{\phi}'|/l_p} \delta_{\alpha\alpha'}$, where $\tilde{\phi}' = \tilde{\phi}(\boldsymbol{\rho}', \boldsymbol{\rho}_{\alpha'})$, l_p is the in-plane correlation length, and σ is the rms roughness length; interhole disorder is assumed uncorrelated.

Our PC membrane has thickness 210 nm, with a triangular lattice of holes of pitch $a = 420$ nm and radius $0.275a$. The waveguide is formed by removing a line of holes. The 1D waveguide band structure for frequencies within the band gap of the 2D PPC is very similar to that shown in Fig. 3(a) of Notomi *et al.* [19]. Recent experi-

ments on a similar structure reported very low loss for PC waveguides (under 1 dB/mm) and clearly demonstrated that the loss is strongly dispersive [5]. To calculate back-scatter loss, we must first, for a given frequency, calculate the field mode profile, wave vector, and group velocity. In Fig. 1 we show the E_y and E_x components of two modes within the lowest-lying (TE-like) propagating band. The normalized wave vector ($2\pi/a$), frequency (c/a), and group index (c/v_g) of these modes are found to be $\bar{k} = 0.4$, $\bar{\omega} = 0.265$ (190 THz), $n_g = 4.7$, and $\bar{k} = 0.32$, $\bar{\omega} = 0.276$ (199 THz), $n_g = 11$. Both of these modes are below the light line and within the photonic band gap.

The computation of the GFT, and thus the total loss, is much more involved. For our calculations, we find the GFT at a range of selected locations along the hole borders. To illustrate some features of the GFT, Fig. 2 shows selected GFT elements for \mathbf{r} near the middle of the slab. In Fig. 2(a) we plot $\text{Im}(G_{xx})$ (solid curve) and $\text{Im}(G_{xy})$ (dashed curve) as a function of frequency for $\mathbf{r} = \mathbf{r}'$. Contained within these curves are precise details regarding the local photon density of states (LDOS) and polarization mixing. One can understand the main features qualitatively, however, by considering the 1D band structure of the propagation modes [19]. The 2D PPC photonic band gap begins at $\bar{\omega} = 0.246$, and there are essentially no waveguiding modes until just below $\bar{\omega} = 0.265$. Thus the xx and xy components are small in this frequency range, as there are essentially no propagation modes into which light can be scattered. Above $\bar{\omega} = 0.265$, however, the lowest-lying (TE-like) propagation band appears, and there is a broad resonance in the two curves of Fig. 2(a) that corresponds directly to this band edge. The higher frequency peaks appear due to an emergence of modes above the light line (radiation modes) and an additional higher order (odd) band with a fairly flat section around $\bar{\omega} = 0.284$.

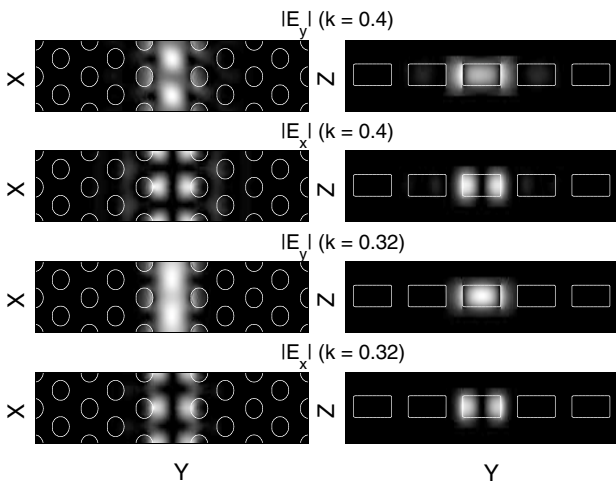


FIG. 1. Example contour plots of the lowest-lying TE-like propagating waveguide mode with normalized wave vector $\bar{k} = 0.32$ and $\bar{k} = 0.4$; the corresponding (normalized) mode frequencies are $\bar{\omega} = 0.276$ ($n_g = 4.7$) and $\bar{\omega} = 0.265$ ($n_g = 11$), respectively.

This frequency dependence of the GFT and the corresponding qualitative description sheds light on the recent dispersive loss measurements [5], namely, that a minimum is expected between the edge of the lowest-lying propagation band and the next TE-like band; only in this region is the LDOS sufficiently small to yield low loss. The frequency dependence of $\text{Im}(G_{yy})$ (solid curve) and $\text{Im}(G_{yx})$ (dashed curve) is also shown, in Fig. 2(b). While similar trends are observed as in Fig. 2(a), the peak at $\bar{\omega} = 0.284$ in $\text{Im}(G_{yy})$ is much more pronounced than that at $\bar{\omega} = 0.265$. To help explain this difference, we examined the spatial GFT components as a function of \mathbf{r}' for various frequencies. We found that near $\bar{\omega} = 0.265$, the xx component was clearly dominated by the $\bar{\omega} = 0.265$ bound mode (i.e., not the radiation modes). This is evident in Fig. 2(c), which shows the spatial profile of $|\text{Im}(G_{xx})|$ at $\bar{\omega} = 0.265$ as a function of x', y' for fixed $z' = z$. At $\bar{\omega} = 0.281$, however, we found that it was the yx component that was dominated by the higher order odd mode, as illustrated in Fig. 2(d), that shows the spatial profile of $|\text{Im}(G_{yx})|$ at $\bar{\omega} = 0.281$.

In Fig. 3(a), we show the dispersion of the total loss that was obtained by calculating Eq. (2) for several modes spanning from $\bar{\omega} = 0.265$ to 0.281, where we chose nominal roughness parameters of $\sigma = 4$ nm and $l_p = 40$ nm. Again, we clearly see a minimum in the region between the edge of the lowest-lying (TE-like) band and the edge of the upper band; this reproduces the loss dispersion trend seen in experiments and agrees with our discussion above. For frequencies even closer to the band edge, recent experiments have shown that the loss increases dramatically. Finally, we examine the role of the rms roughness and correlation lengths on scattering loss. For these calcula-

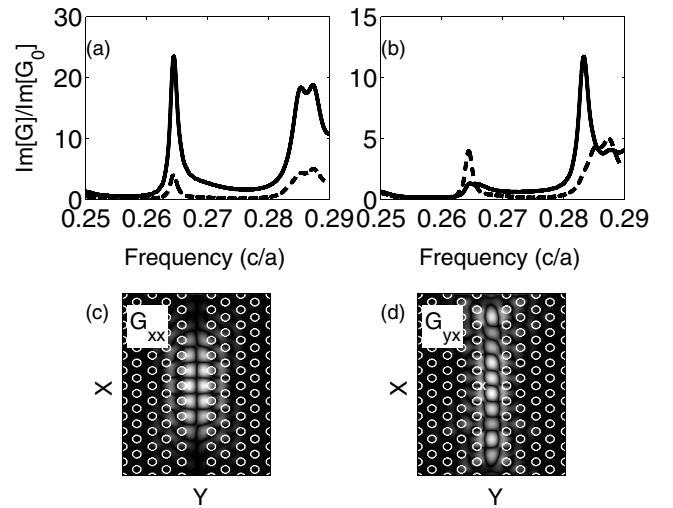


FIG. 2. (a) xx (solid curve) and xy components (dashed curve) of $\text{Im}[\vec{G}^B]$ plotted as a function of frequency, for both \mathbf{r} and \mathbf{r}' fixed at the location indicated by the marked “x” in (c). (b) yy (solid curve) and yx (dashed curve) components at x in (d). The GFT elements are normalized by the free-space Green function. (c) $|\text{Im}[\vec{G}_{xx}]|$ as a function of \mathbf{r}' for \mathbf{r} located at the x , and for $\bar{\omega} = 0.265$. (d) $|\text{Im}[\vec{G}_{yx}]|$, located at x , for $\bar{\omega} = 0.281$.

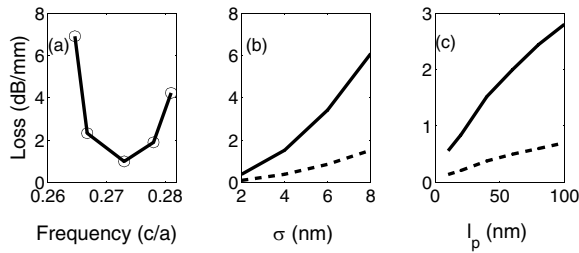


FIG. 3. (a) Total loss as a function of frequency, for $\sigma = 4$ nm and $l_p = 40$ nm. (b) Loss versus the rms roughness σ , corresponding to backscatter loss (solid curve) and total loss (dotted curve), for $l_p = 40$ nm. (c) Loss versus correlation length l_p , for $\sigma = 4$ nm.

tions, we use the propagation mode corresponding to $\bar{k} = 0.36$ and $\bar{\omega} = 0.269$, which is in the low-loss region of Fig. 3(a). We plot the total loss (solid curve) and backscatter loss (dotted curve) as a function of rms roughness length σ in Fig. 3(b) for l_p fixed at 40 nm. We vary σ from 2 to 8 nm and find that the total loss spans about 0.5 to 3 dB/mm. As expected for weak scattering, the loss increases monotonically as a function of roughness size. In Fig. 3(c) we plot backscatter and total loss versus correlation length for $\sigma = 4$ nm. As l_p is increased from 10 to 100 nm, total loss spans from sub-dB/mm to above 6 dB/mm and will saturate as l_p approaches the circumference length of the etched holes, unlike the behavior in Fig. 3(b). Finally, the ratio of backscatter to total loss is highly frequency dependent, and the backscatter loss can be the dominant contribution when v_g becomes sufficiently small.

These low-loss numbers are comparable to *best-of-breed* experimental results, and to obtain them, we have chosen an optimal structure and operating conditions, and extremely good roughness parameters. In general, one may use experiments to fit the disorder parameters, then apply the model with these same parameters to explore a range of other waveguide designs on the same chip; recent comparisons with experiments have already shown this to be very reliable [6]. Although we have made a direct connection to very recent PPC waveguide loss measurements in air-bridge Si [5], the resulting loss numbers (~ 1 dB/mm and below) occur only over a finite bandwidth, well away from other modes and the photonic band edge, and obtaining them requires high quality state-of-the-art fabrication. Loss numbers in the present literature vary substantially. Loss is expected to decrease further as improvements in fabrication are made, and this has been happening recently [21], but we predict that the potentially very serious increase in scattering loss for slow light will, unfortunately, remain a significant problem.

In summary, we have presented a new formalism for the calculation of extrinsic scattering loss in PC waveguides and derived explicit formulas for backscatter loss and total

transmission loss. Rigorous calculations yield loss values comparable to experimental results. In particular, we find that loss becomes unavoidably large for operating frequencies close to the edges of the propagation bands, in agreement with the trends observed in recent measurements. Finally, our general technique can be adopted to describe weak scattering in any arbitrarily shaped optical nanostructure, including photonic crystal nanocavities.

It is a pleasure to thank J. Pond, M.J. Jackson, P. Paddon, M. Warren, M. Povinelli, E. Kuramochi, and M. Notomi for useful discussions.

*Electronic address: hughes@will.brl.ntt.co.jp

†Electronic address: lora.ramunno@science.uottawa.ca

- [1] See, e.g., K. Sakoda, *Optical Properties of Photonic Crystals* (Springer, Berlin, 2001).
- [2] M. Notomi *et al.* IEEE J. Quantum Electron. **38**, 736 (2002).
- [3] C.J.M. Smith *et al.* Appl. Phys. Lett. **77**, 2813 (2000).
- [4] A. Taineau *et al.* Appl. Phys. Lett. **82**, 2577 (2003)
- [5] E. Kuramochi *et al.*, in *Proceedings of the 51st Spring Meeting of the Japan Society of Applied Physics, Hachioji, Japan, 29a-M-5, 2004* (The Japan Society of Applied Physics, Tokyo, 2004), Extended Abstracts No. 3, p. 1146.
- [6] E. Kuramochi *et al.* (to be published).
- [7] A. Chutinan and S. Noda, Phys. Rev. B **62**, 4488 (2000).
- [8] D. Marcuse, Bell Syst. Tech. J. **48**, 3187 (1969).
- [9] F.P. Payne and J.P.R. Lacey, Opt. Quantum Electron. **26**, 977 (1994).
- [10] W. Bogaerts *et al.*, IEEE Photonics Technol. Lett. **13**, 565 (2001).
- [11] Ph. Lalanne and H. Benisty, J. Appl. Phys. **89**, 1512 (2001).
- [12] L. C. Andreani and M. Agio, Appl. Phys. Lett. **82**, 2011 (2003).
- [13] S. Fan, P.R. Villeneuve, and J.D. Joannopoulos, J. Appl. Phys. **78**, 1415 (1995).
- [14] See, for example, T.N. Langtry *et al.*, Phys. Rev. E **68**, 026611 (2003); Kai-Chong Kwan *et al.*, Appl. Phys. Lett. **82**, 4414 (2003).
- [15] W. Bogaerts, P. Bienstman, and R. Baets, Opt. Lett. **28**, 689 (2003).
- [16] Y. Tanaka, T. Asano, Y. Akahane, B.-S. Song, and S. Noda, Appl. Phys. Lett. **82**, 1661 (2003).
- [17] Details of our formalism will be reported in L. Ramunno *et al.* (to be published).
- [18] A contribution in the total loss formula resulting from scattering *into* the forward bound mode may have to be subtracted off. More details will be given in [17].
- [19] M. Notomi *et al.* Phys. Rev. Lett. **87**, 253902 (2001).
- [20] See, for example, A Tafflove, *Computational Electrodynamics: The Finite-Difference Time-Domain Method* (Artech House, Boston, London, 1995).
- [21] S.J. McNab *et al.*, Opt. Express **11**, 2927 (2003); Y. Sugimoto *et al.*, Opt. Express **12**, 1090 (2004); M. Notomi *et al.*, Opt. Express **12**, 1551 (2004).